Compact Design of Dual-band Fractal Ring Antenna for WiMAX and WLAN Applications

Dhirgham K. Naji

Department of Electronic and Communications Engineering, College of Engineering, Al-Nahrain University, Baghdad, Iraq

Abstract This paper proposes a new design approach for dual-band coplanar waveguide (CPW)-fed pentagonal ring fractal patch antenna (PRFPA) which generates two wide resonant frequency bands for -10-dB S_{11} bandwidth to cover 3.5-GHz WiMAX and 5.5-GHz WLAN simultaneously. To achieve dual-band operation, a first-iterative fractal-radiating patch is printed on a single substrate layer and a CPW structure is used to feed this antenna. For numerical analysis, optimization, and electromagnetic (EM) modeling of the prototype structure, CST MWS is used. To assess the antenna performance in terms of impedance bandwidth, radiation pattern, realized peak gain, and efficiency, ANSYS HFSS is employed. Simulation results obtained from the two softwares, having different numerical techniques, are in close agreements, and validate the design principle. The simulation results show that PRFPA has a compact size ($22 \times 22 \times 1.6$ mm^3), planar, simple design and low-cost to be manufactured. In addition, the proposed antenna operates in dual band, it has good stable omnidirectional radiation patterns, and the peak realized gain over the operating bands are 2.04 and 3.44 dB, respectively.

Keywords Coplanar waveguide (CPW), Compact, Dual-band, Pentagonal ring fractal antenna

1. Introduction

Due to the tremendous increasing in modern communication technologies and with the rapid demand for different wireless frequency applications on a single wireless terminal device, compact dual- and multi-band planar antennas are the best solution. Over the past decades, there exist numerous designs of the dual-band planar antennas that based on microstrip technology and have been reported for wireless communications, especially for 3.5-GHz WiMAX (3.3–3.7 GHz), 5.5 GHz (5.150–5.825 GHz) and/or 2.4GHz (2.4–2.483 GHz) WLAN applications [1-7]. These include inverted-F antenna (IFA) structure [1, 2], microstrip line-fed split ring metamaterial structure [3], multiple circular arc-shaped strips with binomial curved conductor-backed plane [4], microstrip line-fed stacked patch antenna [5], multistrip monopole antenna with defected ground structure [6], toothbrush-shaped patch, a meander line, and an inverted U-shaped patch [7]. However, most of these antennas are large in size. Alternatively, asymmetric coplanar strip (ACS)-fed monopole antennas [8-11] have been employed to design compact-size dual-band antennas for WLAN and WiMAX wireless applications. Despite of ACS-fed antennas are capable of providing dual-band with compact size, their

radiation patterns are not symmetrical since the ACS-fed structure has an unbalanced nature [10].

Among feeding structures used for dual-band antennas, the coplanar waveguide (CPW) [12-18] is very attractive by researchers due to its attractive features, such as low profile, low cost and better isolation from feeding networks. In addition, the CPW provides the benefits of good impedance matching, omnidirectional patterns, minimum surface wave and it is easy of fabrication comparing to other excitation methods, e.g. coaxial probe- and microstrip line-fed lines [19]. Thus, based on the aforementioned features of CPW feeding technique, the CPW is adopted here in the design of the proposed antenna.

In general, antennas can operate in different frequency bands by adding and/or modifying either to their radiating patch resonator elements of several distinct lengths depending on the lowest resonance frequency band or etching slots in the ground plane [20]. Although, these antennas have generated multi-band for different applications, but most of them are too complex for the practical applications. Moreover, these antennas result in drawbacks, namely; the use of resonator elements for generating different resonance modes may increase the size of these antennas; mutual coupling among signal paths of different resonator parts; complex fabrication process. Thus, due to the above aforementioned drawbacks of the loading resonator based-technique for dual- and multi-band antenna operation, these antennas are not suitable to use in the case of restricted available terminal space.

Due to the well-known interesting features, self- similarity and space filling, fractal geometries have intrinsic features as compared with traditional Euclidian counterparts for designing miniaturized antennas for multiband wireless applications [21]. Multiband operation have been associated with the characteristic of the self-similarity while miniaturized size is due to the spacing filling property of the fractal geometry [22]. Consequently, miniaturized antennas characterized by good radiation behavior and operation for the desired operational frequency bands could be achieved by utilizing fractal structures for antenna designs.

Nowadays, various forms of fractal structures are used for dual- and multi-band antenna designs [23-26]. For instance, a combination of the Jerusalem cross (JC) as a fractal load and fractal Minkowski slot antenna covering dual-band, 2.4-3.1 GHz and 5.1-5.9 GHz, for WiMAX and WLAN applications, is investigated in [23]. A Koch-like sided Sierpinski hexagonal carpet multifractal monopole antenna fed by CPW with a Koch-like edged fractal ground is proposed in [24], which covers 2.5/3.5/5.5 GHz bands simultaneously. In [25], a novel design of multiband fractal PIFA is considered for dual band operation of antenna by using two folded edges. A CPW-fed slotted Koch snowflake fractal monopole with a U-shaped slot is presented in [26]. It has dual impedance bandwidths covers WLAN bands (2.4/5.2/5.8 GHz) and the WiMAX bands (2.5/3.5/5.5 GHz), respectively. From the literature survey, it is concluded that most of the techniques used for compact-size dual- or multi-band antenna designed have the problems of requiring additional structures, or being complex to be implemented or having large size.

In this paper, we propose a new compact design approach to achieve compact dual-band pentagonal ring fractal patch antenna (PRFPA). The design initially begins with a conventional reference antenna, CPW-fed square patch antenna (SPA). Then intermediate design steps have successfully applied to obtain PRFPA with miniaturized size of 38% compared with the SPA counterpart. In this work, two full-wave available commercially packages are used. All antenna structures are designed and analyzed using finite integration technique (FIT) based CST MWS [27] ver. 2014. In order to verify the CST simulation results of the PRFPA: return loss, radiation pattern, realized peak gain, and efficiency, finite element (FEM) based HFSS [28] ver. 15 is used. A good agreement is shown in the simulation results that offered by the two simulator packages. Thus, this antenna is suitable for WLAN and WiMAX wireless applications.

2. Concept of Dual-band Antenna

This section presents the description of the geometrical configuration of the compact dual-band antenna and outlines the basic four steps of a procedure that applied to antenna designed. A fractal concept based on the first-order pentagonal ring-shaped structure introduces here to achieve optimized dual-band operation of antenna while maintaining compact size. The first step of the procedure begins by designing the reference antenna, CPW-fed SPA, and the final step in the design procedure achieves dual-band antenna, CPW-fed PRFPA.

2.1. Antenna Configuration
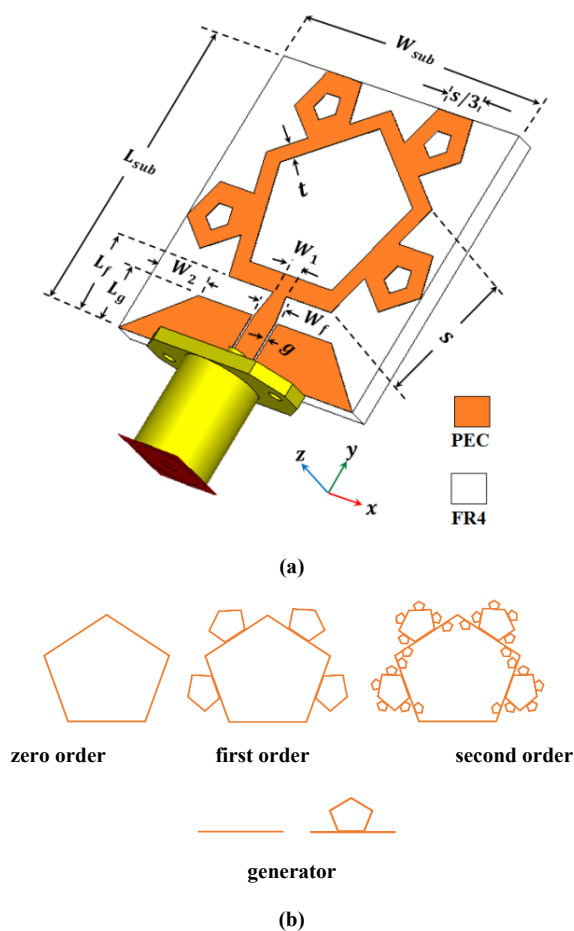
Figure 1. (a) Configuration of the dual-band fractal antenna structure. (b) The recursive-generation procedure for a pentagonal fractal curve. Each perimeter segment of the curve is replaced with the generator. The pentagon structure, initiator or zero order, is shown along with the first two generating iterations

The final geometrical configuration of the proposed antenna is shown in Figure 1(a). This antenna is designed to operate in dual-band, 3.5-GHz WiMAX (3.3-3.7 GHz) and 5.5-GHz WLAN (from 5.150 to 5.825 GHz). The antenna is designed using a square FR-4 substrate with relative permittivity $\varepsilon_r = 4.3$, thickness $h_{sub} = 1.6$ mm and having dimensions $L_{sub} \times W_{sub}$ of 22×22 mm². It comprises of a first iteratively pentagonal ring (PR) fractal-radiating patch, which its recursive-generation procedure is shown in Figure 1(b). The main PR-shaped of the patch (zero-order fractal) has a side length $S = 9.6$ mm, width $t = 1.9$ mm, and it is loaded on its upper four outer edges' centers by four structures of a one-third scaled of the main PR (first-order fractal). A CPW feed has a width $W_f = 2$ mm, length $L_f = 6$ mm and it is terminated with a 50-Ω SMA connector

for signal transmission. The CPW ground has a length $L_g = 4$ mm and the ground is modified by cutting from its upper right corners two pair of triangular-shaped notches, $L_g \times W_2 = 4.0$ mm $\times$ 4.9 mm. This tapered ground plane together with the tapered feeding line dimension, which it is connected to the patch, play a critical key factor of the antenna that dedicates its dual-band functionality.

2.2. Design Procedure

Figures 2 and 3 illustrate the four systematic steps design procedure taken to develop the proposed dual-band antenna, namely:

- Step-1 (SPA and PPA): As for designing dual-band antenna, two wide-band antennas based on CPW-fed are presented. One is a reference antenna, square patch antenna (SPA), and the other is a pentagonal patch antenna (PPA), see Figure 2. They are closely related to each other, and the size and parameter dimension values of them are equal. Initially, and knowing that the size of the antenna is determined approximately by the following formula:

$$L_{sub} = W_{sub} = \frac{c}{2f_l}\left(\frac{\varepsilon_r+1}{2}\right)^{-\frac{1}{2}} \quad (1)$$

where L_{sub} and W_{sub}, the length and width of antenna, respectively, are equal to half of the effective wavelength at f_l, the lowest frequency of operation of antenna. c is the speed of light in free space and ε_r is the dielectric constant of substrate.

Based on (1), we design the SPA by assuming that the thickness of the substrate $h_{sub} = 1.6$ mm, $\varepsilon_r = 4.3$ and $f_l = 3.2$ GHz (the lowest frequency of 3.5-GHz WiMAX band) are given. Then, the SPA is square and has a size $L_{sub} \times W_{sub}$ of 28×28 mm^2.

Figure 2 shows that the patch length L_p and patch width W_p of SPA is related to side length S of the PPA as:

$$L_p = L_{p1} + L_{p2}$$
$$= S \cdot \sin(36°) + S \cdot \sin(72°) \quad (2a)$$

and

$$W_p = W_{p1} + W_{p2}$$
$$= S \cdot \cos(36°) + S \cdot \cos(36°)$$
$$= 2S \cdot \cos(36°) \quad (2b)$$

The optimum performance of the SPA is achieved by the parametric study carried out by CST MWS and the optimized values of antenna dimensions are summarized in Table 1. Based on (2a) and (2b) and a value of $S = 10.8$ mm from simulation, the values of L_p and W_p are 16.6 mm and 17.5 mm, respectively. As a result, return loss, S_{11} curve in Figure 4 shows that SPA has $f_l \cong 3.2$ GHz and highest frequency of operation, $f_h \cong 5.2$ GHz. After SPA is successively designed to cover the 3.5-GHz WiMAX band, then PPA is generated from SPA by subtracting from it the four indicated triangles, 1, 2, 3, and 4, as shown in Figure 2. It is noted from Figure 4 that SPA and PPA S_{11} curves are

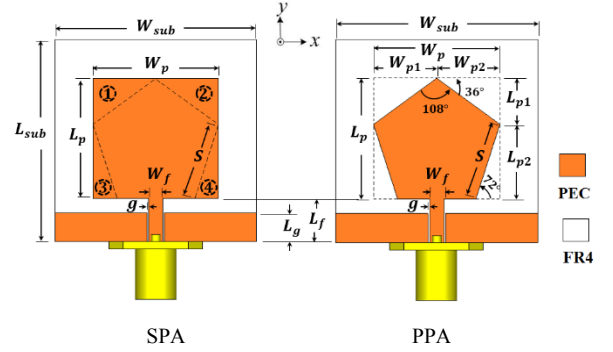nearly similar in term of f_l and they have different values of f_h, 5.2 and 4.6 GHz, respectively.
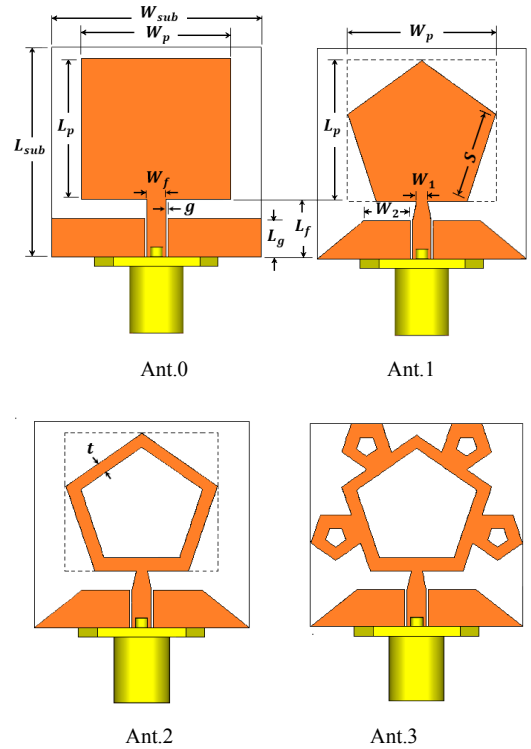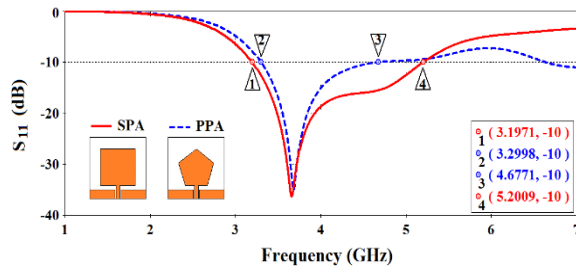

Figure 2.   Geometry of the SPA and PPA

Figure 3.   Geometry of various antennas involved in the design evolution

Table 1.   Antenna design parameter [unit: mm]

Antenna parameter	SPA	PPA
L_{sub}	28	28
W_{sub}	28	28
h_{sub}	1.6	1.6
L_p	16.6	–
W_p	17.5	–
L_g	4.0	4.0
W_f	2.0	2.0
g	0.25	0.25
S	-	10.8

Figure 4. CST simulated return loss, S_{11} curves of SPA and PPA

- Step-2 (Ant.0 and Ant.1): After that SPA and PPA in Step 1 are designed according to the design equations, (1) and (2), miniaturized size of them (Ant.0) and (Ant.1), respectively, see Figure 3, are redesigned by lowering their sizes from $28 \times 28\,\text{mm}^2$ to $22 \times 22\,\text{mm}^2$, i.e., 38% area reduction for each one compared with SPA and PPA counterparts. The comparison in terms of S_{11} plotsfor the intermediate antenna configurations, Ant.0 and Ant.1, besides Ant.2 and Ant.3, obtained from Steps 3 and 4 are illustrated in Figure 5, and the quantitative analysis are summarized in Table 2. It is noticed that for Ant.0 (Ant.1), two resonant modes of 3.9 and 5.3 GHz (3.9 and 6.5 GHz) and single operating band, 3.4-6.0 GHz (two operating bands, 3.5-4.6 GHz and 5.5-lager than7 GHz), are achieved. Due to the dual-band performance of Ant. 2, we need more design steps to achieve the desired operating bands, (3.3-3.7 GHz) WiMAX and (5.150-5.825 GHz) WLAN.

- Step-3 (Ant.2): In this step, Ant.2, zero-order of the pentagonal fractal structure, as Figure 3 shows, is derived by loading the pentagon-shaped patch of Ant.1 by a pentagonal slot at its central portion. The edge of central slot is -scaled of a side length S or the width of the pentagonal ring of Ant.2 is $S/5$. Investigating S_{11} plot in Figure 5, Ant. 2 operates in two bands, 3.30-3.98 GHz and 6.49-6.67 GHz, and has one resonant mode in each band, 3.59 and 6.57 GHz, respectively. It is still needed further design steps (iterative fractals) to bring these two bands of antenna to the required dual-band operation.
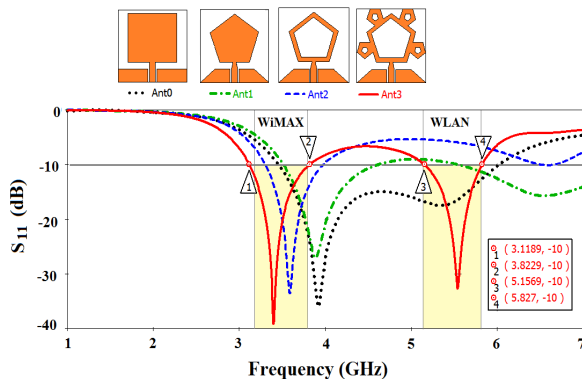
Figure 5. CST simulated return loss curves of various antennas

Table 2. Comparison of intermediate antennas, Ant.0, Ant.1, Ant.2 and Ant.3. Results of SPA and PPA are added for comparison

Antenna	Lower band			Upper band		
	f_l (GHz)	f_h (GHz)	f_r (GHz)	f_l (GHz)	f_h (GHz)	f_r (GHz)
SPA	3.179	5.200	3.644	-	-	-
PPA	3.300	4.677	3.688	-	-	-
Ant.0	3.459	6.026	3.922 5.368	-	-	-
Ant.1	3.515	4.617	3.892	5.541	> 7.0	6.520
Ant.2	3.304	3.980	3.592	6.498	6.677	6.574
Ant.3	3.119	3.823	3.400	5.157	5.827	5.542

Legend: f_l: lowest frequency band, f_h: highest frequency band, f_r: resonance frequency.

- Step-4 (Ant.3): In this final step of a design procedure, the outer four upper edges of the pentagonal patch ring of Ant.2 is loaded with four (1/3)-scaled of pentagonal side length (S). As a result, Ant.3 (first-order fractal) is produced as the proposed antenna. This antenna is operating in the desired dual-band as observed from Figure 5. It is resonates at two resonant frequencies, 3.40 and 5.54 GHz, and covers two bands, 3.119-3.823 GHz and 5.157-5.827 GHz. Hence, Ant.3 is meet the 3.5 and 5.5 GHz frequency and bandwidth specification requirements of WiMAX and WLAN.

3. Results and Discussion

The performance of the proposed antenna is simulated using commercially softwares, namely CST MWS and HFSS. The performance parameters deduced here are return loss, surface current distribution and far-field characteristics, gain, efficiency and radiation patterns.

3.1. Return Loss

Having successfully designed antenna by the procedure described in the previous section and the desired dual-band operation is satisfied, EM simulator based on HFSS is used to validate the result, return loss, obtained by CST MWS. Figure 6 illustrates the S_{11} curve of the proposed antenna, Ant.3 or PRFPA, and its quantitative analysis in terms of f_l, f_h and f_r is listed in Table 3. From Figure 6 and Table 3, a good agreement between two simulation results is observed. A slight difference between the two results can be attributed to different numerical techniques employed by the two simulators.

3.2. Surface Current Distribution

In order to investigate further the return loss performance of Ant.3, the surface current density distribution plots at its two bands' resonant modes, 3.4 and 5.5 GHz, is depicted in Figure 7 using CST. It is observed that most current density is concentrated inside the pentagonal patch radiator, inside the feed line, at the connecting edge of radiating patch and

feed line, and at near edges of ground plane and feed line. As shown in Figure 7, magnetic current density along the patch and the CPW-fed line is getting larger at lower resonant frequency, Figure 7(a), than that at larger resonant frequency, Figure 7(b).
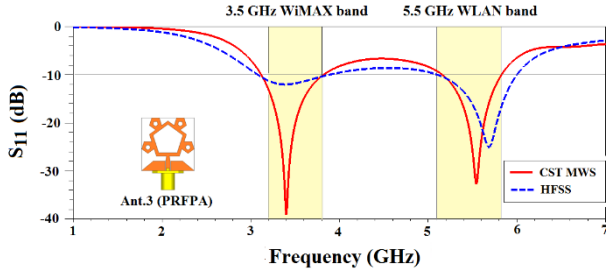

Figure 6. CST and HFSS simulated return loss of the proposed antenna

Table 3. Comparison of CST MWS and HFSS Simulated Results of the proposed antenna, Ant.3 or PRFPA

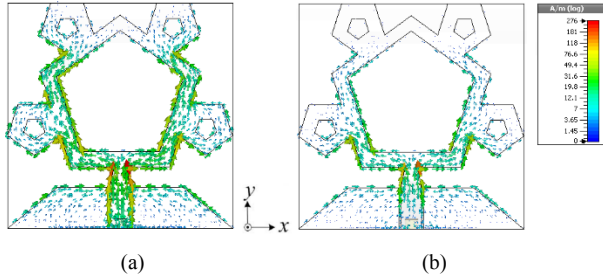| Simulator	Lower band			Upper band		
	f_l (GHz)	f_h (GHz)	f_r (GHz)	f_l (GHz)	f_h (GHz)	f_r (GHz)
CST MWS	3.119	3.823	3.400	5.157	5.827	5.542
HFSS	3.081	3.848	3.406	5.118	6.002	5.680

(a)   (b)

Figure 7. CST simulated results of the surface current distributions for proposed antenna at (a) 3.4 GHz and (b) 5.5 GHz

3.3. Far-field Antenna Performance

Simulated peak-realized gain and efficiency against frequency for the two-resonance frequency bands is shown in Figure 8 and summarize of these results is illustrated in Table 4. Comparison between CST and HFSS results in terms of gain and efficiency as observed show reasonable agreement throughout the aforementioned bands. As Figure 8(a) shows, the CST (HFSS) has a maximum antenna gain of 2.05 dB (1.65 dB) in lower band and 2.44 dB (2.28 dB) in upper band whereas it has a minimum gain of 1.86 dB (1.4 dB) in lower band and 0.71 dB (1.11 dB) in upper band. Part (b) of Figure 8 shows that the efficiency remains above 98.0% (92.0%), 91.4% (93.3%), in the entire lower and upper band, respectively.

The two dimensional (2-D) simulated radiation patterns in the E-plane (yz-plane) and H-plane (xz-plane) at 3.4 and 5.5 GHz are shown in Figure 9. The agreement between the results obtained from the CST and HFSS softwares is quite

apparent. The proposed antenna shows a nearly omnidirectional radiation in the H-plane and bidirectional patterns in the E-plane at two desired operating frequencies. From observing parts (a) and (b) of this figure, the antenna has omnidirectional characteristics over the entire operating frequency bands that is very important for mobile devices.

Table 4. The CST and HFSS simulated realized-peak gain and efficiency of the proposed antenna, Ant.3 or PRFPA

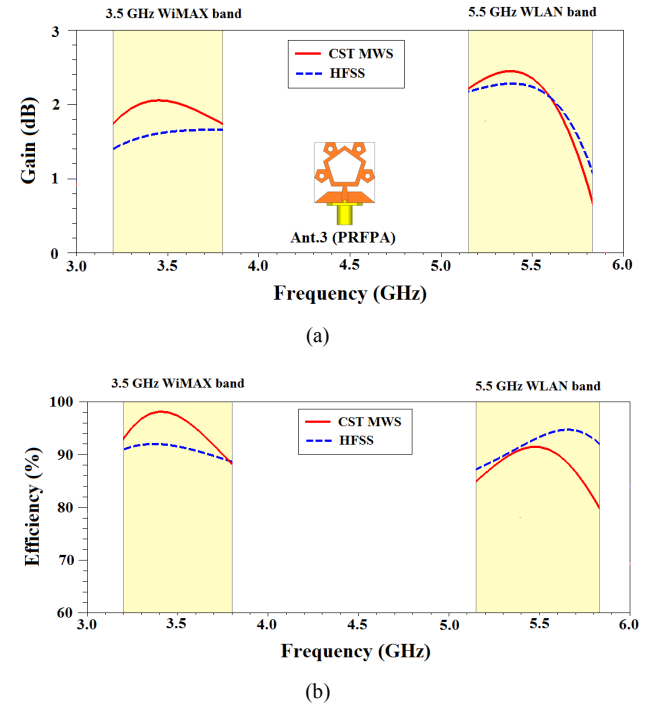| Simulator	@ 3.4 GHz		@ 5.5 GHz	
	Gain (dB)	Efficiency (%100)	Gain (dB)	Efficiency (%100)
CST	2.04	98.0	3.04	91.4
HFSS	1.58	92.0	2.28	93.3

(a)

(b)

Figure 8. CST and HFSS simulated results of (a) gain and (b) efficiency of the proposed antenna

The simulated far-field radiation patterns of the proposed antenna at both resonance frequencies are plotted in Figure 10. As seen, these plots confirm an omnidirectional radiation pattern for both frequencies in H-plane (xz-axis) with radiation nulls in E-plane (yz-axis).

The figure of merit used to measure the quality of the designed antenna in this work is the antenna area reduction factor r_A defined as

$$r_A = \left(1 - \frac{A_{des}}{A_{pub}} \right) \qquad (3)$$

where A_{des} and A_{pub} are the wavelength areas of the designed and published antenna, respectively. Table 5 lists the comparison of our proposed designed antenna with some other antennas that are already reported in literatures in terms of bandwidth, dimensions, and antenna area reduction. This
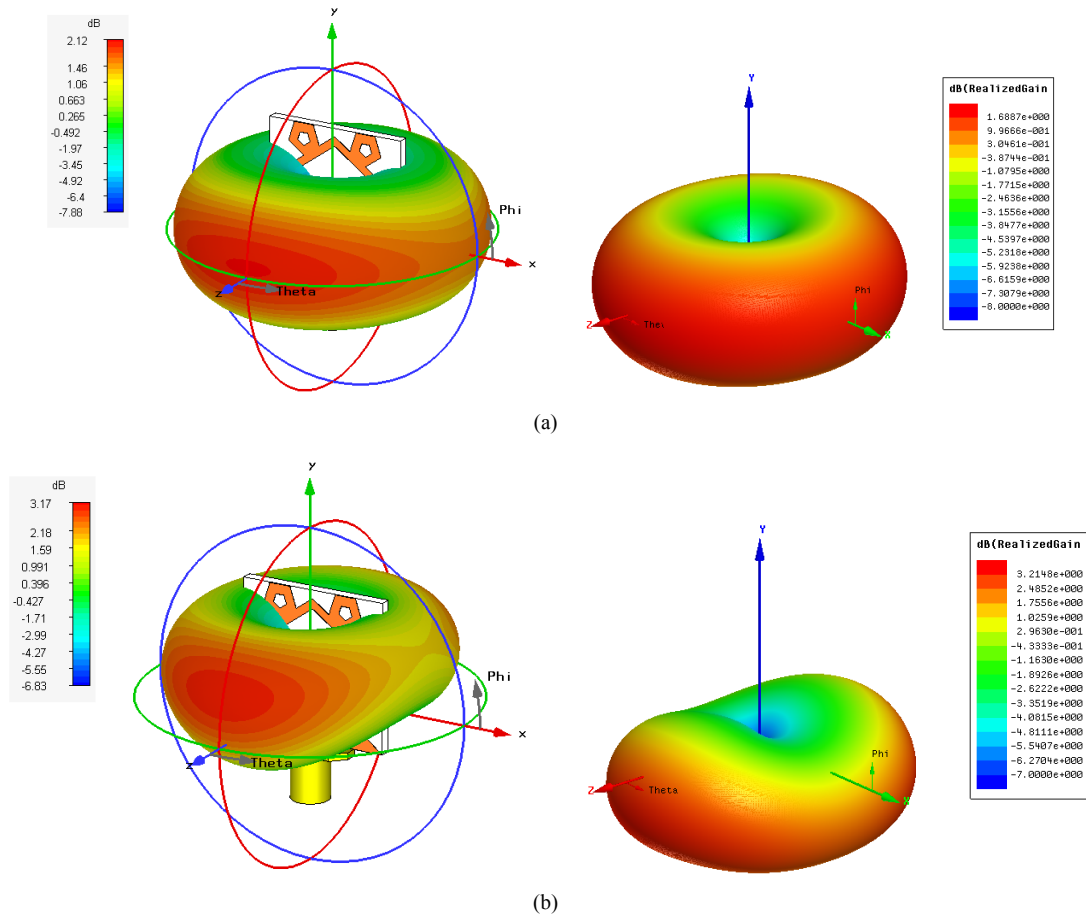
comparison shows that the proposed antenna structure has the smallest area among antenna structures listed in Table 5.

Moreover, developed antenna is suitable for dual-band applications.
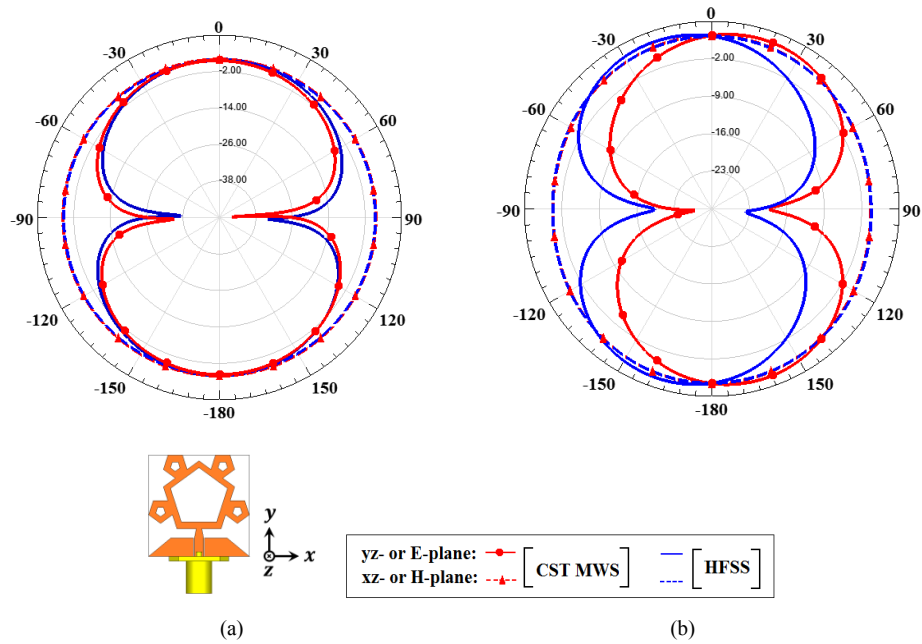
Figure 9. CST MWS and HFSS simulated realized gain in E-plane (yz-plane) and H-plane (xz-plane) at (a) 3.4 and (b) 5.5 GHz

(a)

(b)

Figure 10. CST MWS and HFSSsimulated3-Dfar-field radiation pattern at (a) 3.4 and (b) 5.5 GHz, [left: CST MWS, right: HFSS]

Table 5.   Comparison between the designed antenna and other antennas for WLAN/WiMAX applications

Ref.	Aim	Antenna structure	Bandwidth (GHz)	Area (mm^2)	Area at f_{r1} (λ_{r1}^2)	Area reduction (%)
[5]	compact dual-band antenna, 2.55/5.25 GHz	microstrip line-fed stacked patch antenna	2.40– 2.60 4.90– 5.30	46.4 × 46.4	0.394 × 0.394	57.78
[14]	compact dual-band dual-polarized antenna 2.5/3.5 GHz,	CPW-fed loop slot antenna	2.34 − 2.76 3.22 − 3.88	55 × 57	0.458 × 0.75	69.90
[20]	compact dual-band antenna, 2.4/3.5 GHz	microstrip line loaded with a dumbbell-shaped (DMS) and shorted vias	2.38– 2.52 3.40– 3.62	50 × 30	0.400 × 0.240	31.71
[23]	dual-band antenna, 2.5/5.5 GHz,	T-shaped microstrip line-fed triangular Minkowski fractal slot antenna	2.4– 3.1 5.1– 5.9	40 × 40	0.333 × 0.333	40.90
[24]	triple-band antenna, 2.5/3.5/5.5 GHz	CPW-fed Koch-like sided Sierpinski hexagonal carpet antenna	2.30– 5.85	48 × 40	0.408 × 0.340	52.75
[26]	dual-band antenna, 2.5/3.5/5.5 GHz,	CPW-fed wideband Koch snowflake fractal	2.30– 4.25 4.95– 5.95	41.5 × 27.0	0.346 × 0.225	15.98
[29]	dual-band antenna, 3.5/5.5 GHz,	CPW-fed 9-point star radiating patch antenna	3.05– 3.84 5.24– 7.54	45 × 30	0.525 × 0.350	64.33
[30]	compact triple-band antenna, 2.5/3.5/5.5 GHz	microstrip line-fed modified swastika shape patch antenna	2.28– 3.23 3.28– 3.94 5.05– 6.17	40 × 40	0.333 × 0.333	40.90
[31]	triple-band antenna, 2.5/3.5/5.5 GHz	microstrip line-fed crossed oval-ring slot antenna	2.01– 2.85 3.12– 3.79 5.09– 6.03	55 × 54	0.641 × 0.630	68.20
This work	compact dual-band antenna, 3.4/5.5 GHz	CPW-fed pentagonal ring fractal patch antenna	3.12 − 3.82 5.15 − 5.83	22 × 22	0.256 × 0.256	100.00

Legend: f_{r1}= resonance frequency of the lower band, λ_{r1}= resonance wavelength of the lower band.

4. Conclusions

A dual-band pentagonal-ring fractal patch antenna (PRFPA) has been designed and numerically investigated. With the first-order fractal radiating structure, CPW feeding and tapered ground plane, the proposed antenna can be designed to operate at the 3.5-GHz WiMAX and 5.5-GHz WLAN bands. As required, a new design approach comprising of four systematic steps is introduced to achieve compact dual-band antenna, CPW-fed PRFPA, starting from wide-band reference antenna, CPW-fed square patch antenna (SPA). The proposed antenna designed is characterized by small size (22 × 22 × 1.6 mm^3), 38% reduction in overall size in comparison with the reference antenna.

The CST MWS is used for simulation and investigation of the designed antenna, and the results are confirmed by the aid of HFSS simulation tool. The results obtained from the two EM simulators are in close agreement validating the design concept. Owing to its simple structure, compact size, good radiation performance, and easy to fabricate and integrate with the application-specific circuit boards. This antenna is suitable for use in dual-band band communication systems for WiMAX and WLAN applications.

REFERENCES

[1] C. Y. D. Sim, Y. N. Lai, "An Inverted-F Antenna Design for WLAN/WiMAXDual-Network Applications", *Int. J. RF Microw. Comp.-Aided Eng.*, vol. 24, no. 5, Sept. 2014.

[2] T. Hirano and J. Takada, "Dual-Band Printed Inverted-F Antenna with a Nested Structure", *Progr. In Electromagn. Rese. Lett.,* vol. 61, pp. 1-6, 2016.

[3] Rajesh Kumar V., Raghavan S., "A compact metamaterial inspired triple band antenna for reconfigurable WLAN/WiMAX applications", *AEU Int J. Electron. C,* Iss.One, Vol. 69, pp 274–280, January 2015.

[4] S. Verma, P. Kumar, "Compact arc-shaped antenna with binomial curved conductor-backed plane for multiband wireless applications", *IET Microw. Antennas Propag.*, Vol. 9, Iss. 4, pp. 351–359, 2015.

[5] M. K. Khandelwal, B. K. Kanaujia, S. Dwari, S. Kumar, A.K. Gautam, "Analysis and design of dual band compact stacked Microstrip patch antenna with defected ground structure for WLAN/WiMAX applications", *Int. J. Electron. Comm. (AEU),* vol. 69, pp. 39–47, January 2015.

[6] J. Kaur, R. Khanna and M. Kartikeyan, "Novel dual-band multistrip monopole antenna with defected ground structure for WLAN/IMT/BLUETOOTH/WIMAX applications", *Int. J. Microw. Wirel. Technol.*, pp. 1-8, 2013.

[7] Yingsong Li and Wenhua Yu, "A Miniaturized Triple Band Monopole Antenna for WLAN and WiMAX Applications", *Int. J. Antennas Propag.,* pp. 1-5, Oct. 2015.

[8] Li, Y., Li, W., & Mittra, R., "A compact ACS-fed dual-band meandered monopole antenna for WLAN and WiMAX applications", *Microw. Opt. Technol. Lett.*, 55, 2370–2373, 2013.

[9] Li, Y., Li, W., & Ye, Q., "A compact asymmetric coplanar strip-fed dual-band antenna for 2.4/ 5.8 GHz WLAN applications", *Microw. Opt. Technol. Lett.*, vol. 55, pp. 2066–2070, 2013.

[10] X. Li, X.-W. Shi, W.-Hu, P. Fei, and J.-F. Yu, "Compact Triband ACS-Fed Monopole Antenna Employing Open-Ended Slots for Wireless Communication", *IEEE Antennas and Wirel. Propag. Lett.*, vol. 12, pp. 888-391, 2013.

[11] Praveen V. Naidu and Raj Kumar, "Design of a Compact ACS-Fed Dual Band Antenna for Bluetooth/WLAN and WiMAX Applications", *Progr. In Electromagn. Res. C*, vol. 55, pp. 63–72, 2014.

[12] Z. Hamouda, J.-L. Wojkiewicz, A. A. Pud, L. Kone, B. Belaabed, S. Bergheul, and T. Lasri, "Dual-Band Elliptical Planar Conductive Polymer Antenna Printed on a Flexible Substrate", *IEEE Trans. Antennas and Propag.*, vol. 63, no. 12, pp. 5864-5867, Dec. 2015

[13] W.-C. Liu, C.-M. Wu, and N.-C. Chu, "A compact CPW-fed slotted patch antenna for dual-band operation", *IEEE Antennas and Wirel. Propag. Lett.*, vol. 9, pp. 110-113, 2010.

[14] M.-T. Tan, B.-Z. Wang, "A compact dual-band dual-polarized loop-slot planar antenna", *IEEE Antennas and Wireless Propag. Lett.*, vol. 14, pp. 1742-1745, 2015.

[15] M.-T. Wu, M.-L. Chuang, "Multibroadband slotted bow-tie monopole antenna", *IEEE Antennas and Wirel. Propag. Lett.,* vol. 14, pp. 887-890, 2015.

[16] R.-Z. Wu;P. Wang, Q. Zheng,R.-P. Li, "CompactCPW-fed triple-band antenna for diversity applications", *Electron. Lett.,*vol. 51,Iss. 4, pp. 735-736, 2015.

[17] S. S. Huang, J. Li, and J. Z. Zhao, "Compact CPW-fed tri-Band antenna for WLAN/WiMAX applications", *Progr. In Electromagn. Res. C*, vol. 49, pp. 39–45, 2014.

[18] B. Li, Z.-H. Yan, T.-L. Zhang C. Wang, "A compact tri-bandpatch antenna with notched ground for WLAN/WiMAX communication", *J. Electromagn. Waves and Applications*, vol.27, Iss. 2, pp.250-256, 2013.

[19] D. K. Naji, "An alternative look to design of wideband planar monopole antennas based on parasitic elements for C-band wireless applications", *Int. J. Electromagn. Applications,* vol. 4, no. 3, pp. 61-69, 2014.

[20] J. Malik, A. Patnaik, and M. V. Kartikeyan, "A compact dual-band antenna with omnidirectional radiation pattern", *IEEE Antennas and Wirel. Propag. Lett.,* vol. 14, pp. 503-506, 2015.

[21] D. H. Werner, S. Ganguly, "An overview of fractal antennas engineering research", *IEEE Antenna Propag. Mag.*, vol. 45, pp. 38–56, 2003.

[22] M. Rahimi, S. Heydari, Z. Mansouri, N. P. Gandji, and F. B. Zarrab, "Investigation and design of an ultra-wideband fractal ring antenna for notch applications", *Microw. Opt. Technol. Lett.*, vol. 58, no. 7, pp. 1629–1634, July 2016.

[23] M. S. Sedghi, M. N.-Moghadasi, and F. B. Zarrabi, "A dual band fractal slot antenna loaded with Jerusalem crosses for wireless and WiMAX Communications", *Progr. In Electromagn. Res. Lett.,* vol. 61, pp. 19–24, 2016.

[24] D. Li,J.-F. Mao, "Coplanar waveguide-fed Koch-like sided Sierpinski hexagonal carpet multifractal monopole antenna", *IET Microw., Antennas Propag.*, Vol. 8,Iss. 5, pp. 358 – 366, 2014.

[25] N. Saluja, and R. Khanna, "Design, analysis, and fabrication of a novel multiband folded edge compact size fractal PIFA for WIFI/LTE/WIMAX/WLAN application", *Micro. Opt. Technology. Lett.*, vol. 56, no. 12, pp. 2836–2841, Dec. 2014.

[26] D. Li, F.-S. Zhang, Z.-N. Zhao, L.-T. Ma, and X.-N. Li, "A CPW-fed wideband Koch snowflake fractal monopole for WLAN/WiMAX applications", *Progr. In Electromagn. Res.C*, vol. 28, pp. 143-153, 2012.

[27] CST Inc, CST Microwave Studio Suite 2014. (2014).

[28] High Frequency Structure Simulator (HFSS) Ansoft ver. 15, 2015.

[29] T. Mandal, S. Das, "Coplanar waveguide fed 9-point star shape monopole antennas for worldwide interoperability for microwave access and wireless local area network applications", *J. Eng.*, pp. 1-5, 2014.

[30] M. Samsuzzaman, T. Islam, N. H. Abd Rahman, M. R. I. Faruque, and J. S. Mandeep, "Compact Modified Swastika Shape Patch Antenna for WLAN/WiMAX Applications", *Int. J. Antennas and Propag,* Volume 2014, Article ID 825697, 8 pages.

[31] D.-S. Cai, Z.-Y. Lei, H. Chen, G.-L. Ning, and R.-B. Wang, "Crossed oval-ring slot antenna with triple-band operation for WLAN/WIMAX applications", *Progr. In Electromagn. Res. Lett.*, Vol. 27, pp. 141–150, 2011.